Table I. Permeability and Selectivity Coefficients for Various Gases in Polycationic (PMPy-NO_3) and Neutral[a] (PMPy) Poly(*N*-methylpyrrole) Films

polym	P_{O_2}[b]	P_{N_2}	α_{O_2/N_2}[c]	P_{CO_2}	P_{CH_4}	α_{CO_2/CH_4}
PMPy-NO_3	1.26	0.16	7.9	2.82	0.17	16.2
PMPy	2.04	0.33	6.2	6.90	0.22	31.9

[a] PMPy was prepared by treating PMPy-NO_3 with 0.005 M $NaBH_4$ in CH_3CN. [b] Permeability coefficients in Barrers = 10^{-10} cm^3 (STP) cm/cm^2 s cmHg. Membrane area was 0.0792 cm^2. Pressure differential was 50 psi. Film thickness was 1.4 μm. [c] Ratio of permeability coefficients. See text.

contacted the equilibrium vapor associated with the neat monomer.

Because the membrane is hydrophobic,[9] the $Fe(NO_3)_3$ solution cannot flood the pores. Monomer vapor can, however, permeate the pores and react[4a,b] with the Fe^{3+} at the membrane/solution (opposite) interface (Figure 1). This caused a thin, strongly adherent film of the ECP to "grow" across the membrane surface. We have used this method to form Anopore/ECP composite membranes based on polypyrrole, polythiophene, poly(3-methylthiophene), and poly(*N*-methylpyrrole). A scanning electron micrograph of a typical composite membrane is shown in Figure 2. Film thickness can be conveniently controlled by varying the duration of the polymerization period.

The majority of our gas-transport data, to date, have been obtained on composites based on polypyrrole (PPy) and poly(*N*-methylpyrrole) (PMPy). Gas-transport data were obtained by using the single gas-permeation method.[7,11] This method provides the permeability coefficient (P_g) for the gas in the thin ECP film.[11] The permeability coefficients for two gases can then be ratioed to yield the selectivity coefficient (α).[11]

Table I shows P_g and α values for various gases in two PMPy films; the films were 1.4 μm thick. This table contains an enormous quantity of information. First, these data show that these thin films are essentially defect-free. If microscopic defects, or pores, were present in these films, gas would be transported through these defects via Knudson flow.[2] If this mechanism predominated, the O_2/N_2 selectivity coefficient ($\alpha_{O/N}$) would be 0.94; furthermore, even minute numbers of defects cause Knudson flow to predominate.[2] The high (vide infra) $\alpha_{O/N}$ values shown in Table I indicate that these thin PMPy films are essentially defect-free. This is extremely important to separations applications of such membranes because defects destroy chemical selectivity.[2] It is of interest to note that we have conducted analogous studies on PPy-NO_3 and these films show Knudson selectivity coefficients. Thus, in contrast to PMPy-NO_3, PPy-NO_3 appears to be porous.

Second, we raised the interesting possibility of using the polyionic to neutral-polymer transition[4] to reversibly alter the gas-transport properties of an ECP film. Table I indicates that this is an experimental reality. Note that the P_g values for all gases in the polycationic form of PMPy are lower than the P_g's for the neutral form of this polymer. It is well-known that introduction of ionic groups into a polymer lowers the available void volume.[12] This decrease in void volume is undoubtedly responsible for the diminution in the P_g values for PMPy-NO_3.

Finally, Table I shows that PMPy-NO_3 has extraordinary gas-transport characteristics. One of the highest $\alpha_{O/N}$ to be reported in the literature, to date, is a value of 8.0 for poly(*p*-hydroxystyrene).[11b] PMPy-NO_3 essentially matches this exceptional selectivity (Table I). However, the P_gs for O_2 and N_2 in PMPy-NO_3 are an *order of magnitude higher* than in poly(*p*-hydroxystyrene).[11b] Thus, PMPy-NO_3 provides both high selectivity and high flux. This is an important observation because enhanced selectivity in a polymer film can usually be achieved only at the expense of flux.[11b] PMPy-NO_3 appears to be an exception to this general rule and thus shows potential for use as a high-performance material in gas-separation systems.

We are currently attempting to elucidate the chemical basis for these extraordinary gas-transport characteristics. We have obtained analogous results from a highly sulfonated styrenic polymer.[3b] We believe, therefore, that the high ion content of these materials is a critical factor.[3b] Furthermore, ECPs provide a wealth of opportunities for fundamental investigations of the effects of molecular and supermolecular structure on gas transport in polymers. Polymers with a large variety of chemical structures and substituents can be easily synthesized,[13] and the counterion in the doped form can be changed, at will, via ion exchange. We are currently exploring these unique opportunities.

Acknowledgment. This work was supported by the Air Force Office of Scientific Research. We thank Chao Liu for constructing the gas-permeation apparatus.

Registry No. PPy, 30604-81-0; PMPy, 72945-66-5; NO_3, 14797-55-8; O_2, 7782-44-7; N_2, 7727-37-9; CO_2, 124-38-9; CH_4, 74-82-8; Anopore, 127361-04-0.

(11) (a) Koros, W. J.; Chan, A. H.; Paul, D. R. *J. Membr. Sci.* **1977**, *2*, 165. (b) Puleo, A. C.; Muruganandam, N.; Paul, D. R. *J. Polym. Sci. Part B: Polym. Phys. ed.* **1989**, *27*, 2385.

(12) Eisenberg, A.; Hird, B.; Moore, R. B., III *Macromolecules* **1990**, *23*, 4098.

(13) Skotheim, T. A., Ed. *Handbook of Conductive Polymers*; Marcel Dekker: New York, 1986.

Growth of Free-Standing Diamond Films on Glass

Khushrav E. Nariman,[†] D. Bruce Chase,[‡] and Henry C. Foley*,[†,§]

Center for Catalytic Science and Technology
Department of Chemical Engineering
Department of Chemistry and Biochemistry
University of Delaware, Newark, Delaware 19716
Central Research and Development
E. I. du Pont de Nemours & Co.
Wilmington, Delaware 19898

Received January 25, 1991
Revised Manuscript Received March 18, 1991

The unique properties possessed by diamond make it extremely attractive for various materials applications.[1,2] In addition to being the hardest material available (Mohs hardness = 10) it also has the highest thermal conductivity (~20 W cm^{-1} K^{-1}) and a large optical bandgap (5.5 eV). The bandgap provides transparency in the high-frequency region of the spectrum. Hence free-standing films of di-

[†] Center for Catalytic Science and Technology.
[‡] E. I. du Pont de Nemours & Co.
[§] Department of Chemistry and Biochemistry.
* Author to whom correspondence should be addressed.

(1) Weast, R. C., Ed. *CRC Handbook of Chemistry and Physics*; CRC Press Inc.: Boca Raton, FL, 1989.

(2) Field, J. E. *Properties of Diamond*; Academic Press: London, 1979; p 647.

0897-4756/91/2803-0391$02.50/0

amond have potential uses as X-ray windows. (Natural diamond is used in X-ray windows at present.) For this purpose, chemical vapor deposition (CVD) of diamond films needs to be done on a substrate from which the film can be separated. Silicon is one such substrate, and due to the close similarity of its crystal structure with that of diamond (both possess the diamond crystal lattice, with lattice parameter values of: $a_{0,silicon}$ = 5.4305 Å, $a_{0,diamond}$ = 3.5670 Å) growth rates of diamond on silicon are high.[3] However, the film also adheres extremely well to the substrate and the silicon needs to be etched away (using HF) to obtain a free-standing diamond film. Clearly, it would be advantageous to grow diamond on a substrate to which it does not adhere, since the film simply could be lifted off the substrate. In this communication we report the synthesis of pure, polycrystalline diamond films that are free-standing and easily removed from a glass substrate.

We have demonstrated that it is possible to grow a film that lifts off easily, on Corning type 7059 glass, presumably because of the large difference in the thermal expansion coefficients between glass and diamond. The main difficulty in growing diamond on such a substrate is that glass cannot withstand temperatures in excess of 600 °C and so the deposition process employed must not result in excessive heating of the substrate. Most of the reported plasma-enhanced deposition processes employed for diamond growth operate at substrate temperatures in the 700–1000 °C[4-8] range, well out of the useful range for growth of diamond on glass. As part of our investigations into the growth of novel diamond materials, we utilize a voltage-biased, hot-filament deposition process that is capable of growing diamond at substrate temperatures of less than 500 °C.[9]

The reactor consists of a six-way stainless steel cross, connected to a turbo- and backing-pump combination capable of attaining an ultimate vacuum of 10^{-5} Torr. In these experiments, the reaction chamber was pumped-down to a pressure of $<10^{-4}$ Torr, and then the pressure was raised to 25 Torr by allowing the reactant gases into the chamber. Pressure was maintained at 25 Torr by using a pressure controller and leak-valve assembly.

After being cleaned with a detergent solution, distilled water, and acetone, the Corning type 7059 glass substrate (2.5 × 2.5 × 0.8 cm) was dried in air and scratched with 0.5-μm diamond dust. This was done to seed the growth of the diamond film. Excess diamond dust was removed with high-pressure air. The seeded glass substrate was placed on a stainless steel base and heated exclusively by radiation from the filament. A K-type thermocouple placed above and in contact with the substrate showed that it attained a temperature of ~400–500 °C. The filament consisted of a hand-wound tungsten wire supported on a holder that is heated to 2000–2400 °C (as measured by an optical pyrometer) by passing a current of ~15 A through it. A negative potential bias of 50–100 V was applied to the filament to increase electron emission and enhance electron bombardment of the substrate and growing film. The reactant gases methane (UHP, 99.97% minimum) and hydrogen (UHP, 99.999% minimum) were fed into the reactor through mass flow controllers with mixing occurring prior to entry into the system. The mixed reactant gases flowed through an inlet nozzle that consists of a 0.6-cm-i.d. stainless-steel tube held 2.5 cm from the substrate.

This arrangement resulted in nearly line-of-sight deposition on the substrate. Methane concentrations in hydrogen were varied from 0.5% to 5%. Higher CH_4 concentrations resulted in higher overall deposition rates, but the film quality deteriorated since its graphitic content also increased. A concentration of 1% CH_4 in H_2 provided growth-rates of approximately 1 μm/h. This rate was estimated by making a film thickness measurement on a cleaved film using a scanning electron microscope (Figure 1, top). Growth on the seeded surface was found to be much higher than on an unseeded one. Scanning electron micrographs of the seeded substrate showed several microfine scratches on the glass surface along with some diamond crystallites that appear rounded rather than faceted due to the milling process used in their manufacture.

The adhesion behavior of the diamond film on glass showed that films thinner than ~1.5 μm adhered quite well to the glass substrate and could not be removed by scratching with a stainless steel tip. However, films thicker than 2–2.5 μm tended to flake off. A likely reason for this is the difference in the thermal expansion coefficients between glass (3.2×10^{-6} °C^{-1}) and diamond (1.2×10^{-6} °C^{-1}).[10] The adhesion mechanism is not known; however, the graphitic carbon that forms along with diamond and that is not etched away by hydrogen atoms may play a role in weakly bonding the diamond to glass surface. This is further substantiated by scanning electron microscopy of the film. Micrographs of the side of the film in contact with the glass substrate do not show the presence of crystallites, even with a magnification of up to 40 000×. On the other hand, the outer surface of the diamond film (Figure 1, bottom) shows pronounced crystallites in habits typical of hot-filament growth. Fourier transform laser Raman spectroscopy performed on the "free-standing" film (Figure 2) shows the characteristic peak due to sp^3 diamond carbon at 1332 cm^{-1}. It is noted however that the surface of the film in contact with the glass is darker in color, presumably because of a larger proportion of graphitic inclusions in that region compared to the outer surface.

These data point out that the initial stages of deposition are critical since the amount of non-diamond carbon incorporated is largely controlled by conditions early on in the deposition. A possible explanation for this occurrence derives from the growth conditions in the hot-filament reaction. Since the substrate is not heated externally, it is relatively cold in the initial stages of the deposition. Assuming that diamond growth occurs via simultaneous deposition and etching of both the diamond and graphitic phases as postulated by Derjaguin and co-workers, it is likely that the etch rate for the graphitic phase is low at the low initial temperatures.[11] As a result, there is a rapid buildup of a graphitic layer in the early stages of the deposition, which occurs simultaneously with the growth of

(3) DeVries, R. C. *Annu. Rev. Mater. Sci.* **1987**, *87*, 161.
(4) Spitsyn, B. V.; Bouilov, L. L.; Derjaguin, B. V. *J. Cryst. Growth* **1981**, *52*, 219.
(5) Badzian, A. R.; Badzian, T.; Roy, R.; Messier, R.; Spear, K. E. *Mater. Res. Bull.* **1988**, *23*, 531.
(6) Badzian, A. R.; DeVries, R. C. *Mater. Res. Bull.* **1988**, *23*, 385.
(7) Kobashi, K.; Nishimura, K.; Miyata, K.; Kumagai, K.; Nakaue, A. *J. Mater. Res.* **1990**, *5*, 2469.
(8) Matsumoto, S.; Sato, Y.; Kamo, M.; Setaka, N. *Jpn. J. Appl. Phys.* **1982**, *21*, L183.
(9) Nariman, K. E.; Saito, A.; Foley, H. C. *Synthesis and Properties of New Catalysts: Utilization of Novel Materials Components and Synthetic Techniques*; Corcoran, E. W., Jr., Ledoux, M. J., Eds.; *Mater. Res. Soc. Extended Abstr.* **1990**, *EA*-24, Pittsburgh, PA.
(10) Perry, R. H., Green, D. W., Maloney, J. O., Eds. *Perry's Chemical Engineer's Handbook*, 6th. ed.; McGraw-Hill: New York 1984.
(11) Derjaguin, B. V.; Fedoseev, D. V. *Growth of Diamond and Graphite from the Gas Phase*; Nauka: Moscow, 1977.

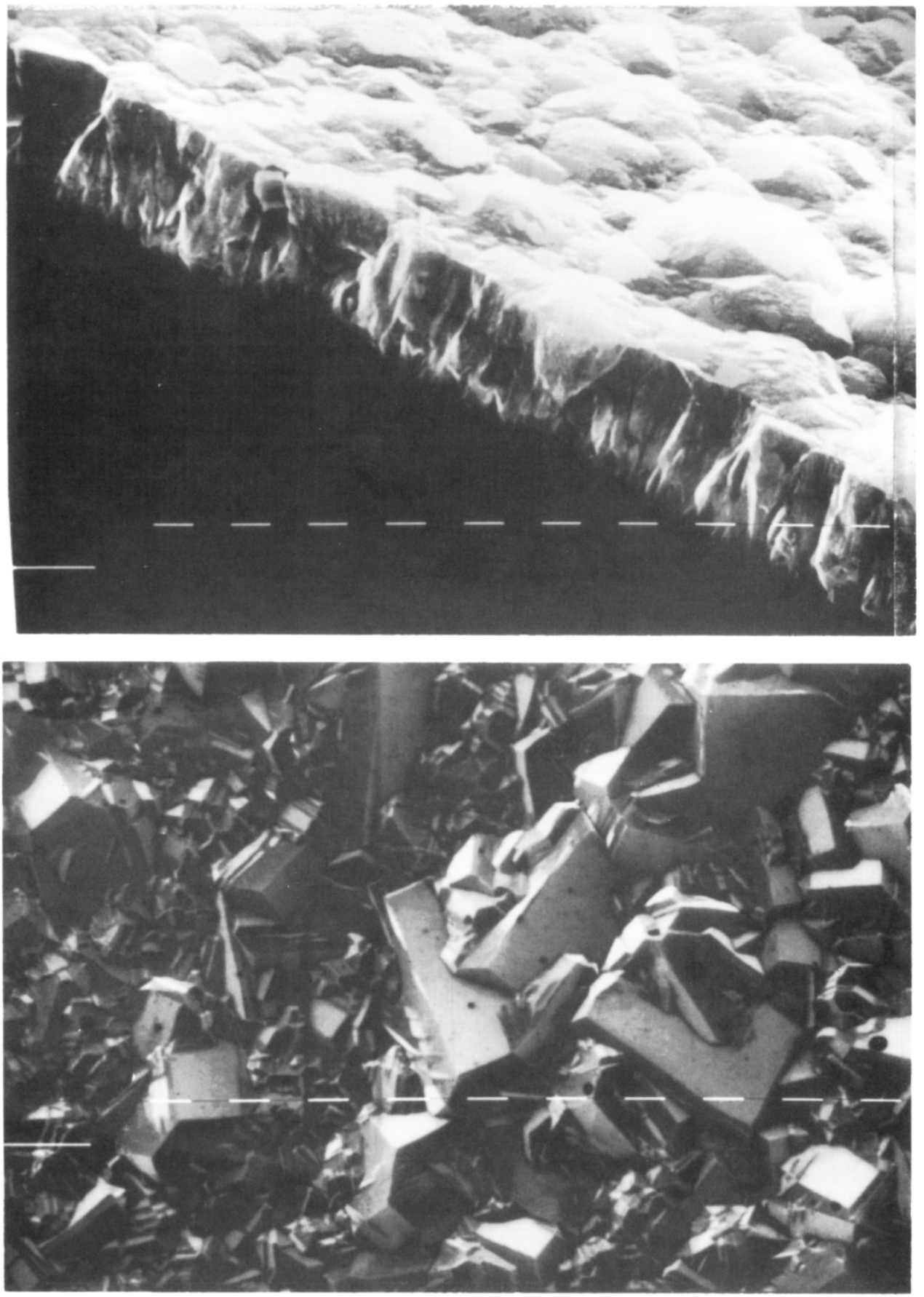

Figure 1. Top: scanning electron micrograph of a cross section of the free-standing film, showing columnar growth of the diamond crystallites (1-μm markers). Bottom: scanning electron micrograph of the outer growing surface of the free-standing diamond film. Multiply nucleated crystallites are visible, with predominant (100) crystal faces (1-μm markers).

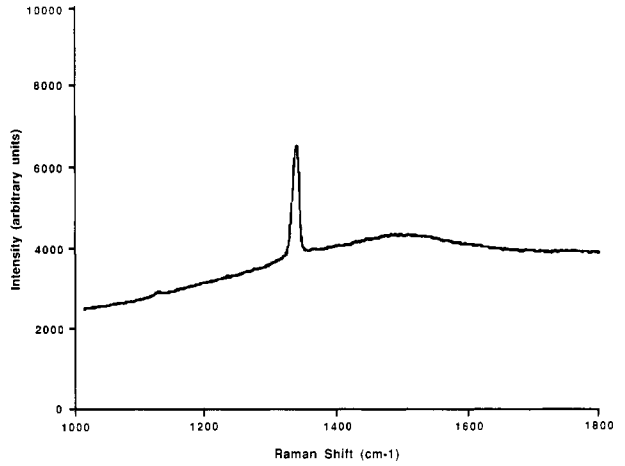

Figure 2. Raman spectrum of the free-standing film showing the characteristic peak for diamond at 1332 cm^{-1}. The shoulder at ~1550 cm^{-1} is virtually absent, indicating compositional purity.

diamond. This graphitic carbon lowers the overall purity and quality of the diamond film. Similar effects may occur in the growth of CVD diamond on other substrates.

To avoid the formation of an excessively graphitic deposit in the initial stages of the deposition, an experimental run was performed with an altered sequence of events. The reactor was pumped down to 10^{-4} Torr as before, but instead of flowing both H_2 and CH_4 simultaneously to raise the pressure to 25 Torr, only H_2 was used. Next the filament was heated to glowing in pure H_2 and then the CH_4 flow was initiated, well after the filament and substrate temperatures were stabilized. This resulted in films that appeared lighter in color on the glass side.

In conclusion, we have demonstrated that it is possible to grow diamond on a nonadhering, amorphous substrate, in this case glass, and this approach provides an entree into the growth of better free-standing films of diamond with macrostructures designed for particular applications. In addition, the morphological and compositional differences in the film adjacent to the glass substrate as compared to that on the outer surface have been noted, and a possible reason for these has been postulated, which may have vital consequences for diamond growth on other substrates.

Acknowledgment. H.C.F. thanks the National Science Foundation for support of this work through the Presidential Young Investigator award (CBT-No. 8657614). We express our thanks to Central Research and Development at Du Pont for the use of the Raman spectrometer.

Registry No. C, 7782-40-3.

Reviews

Chemical Amplification Mechanisms for Microlithography

E. Reichmanis,* F. M. Houlihan, O. Nalamasu, and T. X. Neenan

AT&T Bell Laboratories, Murray Hill, New Jersey 07974

Received October 12, 1990. Revised Manuscript Received March 8, 1991

Continued advances in microelectronic device fabrication are trying the limits of conventional lithographic techniques. In particular, conventional photoresist materials are not appropriate for use with the new technologies that will be necessary for sub-0.5-μm lithography. One approach to the design of new resist chemistries involves the concept of chemical amplification, where one photochemical event can lead to a cascade of subsequent reactions that allow patterning of the parent material. Generally, chemically amplified resists utilize photochemically generated acid to catalyze cross-linking or deprotection reactions. This paper reviews the chemistries that have been evaluated for chemical amplification resist processes; acid generator, cross-linking, deprotection, and depolymerization chemistry.

Introduction

A modern integrated circuit is a complex three-dimensional structure of alternating, patterned layers of conductors, dielectrics, and semiconductor films. This structure is fabricated on an ultrahigh-purity substrate of a semiconducting material such as silicon. The performance of the device is, to a large degree, governed by the size of the individual circuit elements. As a general rule, the smaller the elements, the faster the device and the more operations it can perform. The device structure is produced by a series of steps used to pattern each layer precisely.[1,2] The patterns are formed by lithographic processes that consist of two steps: (1) delineation of the patterns in a thin radiation-sensitive polymer film (resist); (2) transfer of that pattern into the substrate using an appropriate etching technique. A schematic representation of the lithographic process is shown in Figure 1.

Significant advances are continually being made in microelectronic device fabrication and, especially in lithography, the technique that is used to generate the high-resolution circuit elements characteristic of today's integrated circuits. Fifteen years ago, the state-of-the-art device contained up to 8000 transistor elements and had 5–6-μm minimum features. Today, devices with several million transistor cells are commercially available and are fabricated with minimum features in the range of 0.8 μm.[3,4]

(1) Sze, S. M. *VLSI Technology*; McGraw-Hill: New York, 1983.
(2) Wolf, S.; Tauber, R. N. *Silicon Processing for the VLSI Era*; Lattice Press: Sunset Beach, CA, 1986.
(3) *Electronic and Photonic Applications of Polymers*; ACS Advances in Chemistry Series, No. 218; Bowden, M. J., Turner, S. R., Eds.; American Chemical Society: Washington, D.C., 1988.

0897-4756/91/2803-0394$02.50/0